Impact of slepton generation mixing on the search for sneutrinos

A. Bartl[a], K. Hidaka[b], K. Hohenwarter-Sodek[a], T. Kernreiter[a], W. Majerotto[c] and W. Porod[d]

[a] *Faculty of Physics, University of Vienna, Boltzmanngasse 5, A-1090 Wien, Austria*
[b] *Department of Physics, Tokyo Gakugei University, Koganei, Tokyo 184–8501, Japan*
[c] *Institut für Hochenergiephysik der Österreichischen Akademie der Wissenschaften, A-1050 Vienna, Austria*
[d] *Institut für Theoretische Physik and Astrophysik, Universität Würzburg, D-97074 Würzburg, Germany*

Abstract

We perform a systematic study of sneutrino production and decays in the Minimal Supersymmetric Standard Model (MSSM) with slepton generation mixing. We study both fermionic decays like $\tilde{\nu} \to \ell^- \tilde{\chi}^+, \nu \tilde{\chi}^0$ and bosonic decays such as $\tilde{\nu} \to \tilde{\ell}^- H^+, \tilde{\ell}^- W^+$. We show that the effect of slepton generation mixing on the sneutrino production cross sections and its decay branching ratios can be quite large in a significant part of the MSSM parameter space despite the very strong experimental limits on lepton flavour violating processes. This could have an important impact on the search for sneutrinos and the determination of the MSSM parameters at future colliders, such as LHC, ILC, CLIC and muon collider.

1 Introduction

In the Minimal Supersymmetric Standard Model (MSSM) [1], supersymmetric (SUSY) partners of all Standard Model (SM) particles with masses less than $\mathcal{O}(1\text{ TeV})$ are introduced. In this way, SUSY solves the problems of hierarchy, fine-tuning and naturalness of the SM. Hence, the discovery of the SUSY partners and the study of their properties play an important role at future colliders, such as the Large Hadron Collider (LHC), e^+e^- linear colliders (ILC and CLIC), and $\mu^+\mu^-$ collider. They will extend the discovery potential for SUSY particles to the TeV mass range, and allow for a precise determination of the SUSY parameters.

In this letter we focus on the sneutrinos, the SUSY partners of neutrinos. Systematic studies of sneutrino decays in the MSSM including the effects of CP violation have been performed already [2, 3]. In these studies it has been assumed that individual lepton flavour is conserved in the slepton sector, which is suggested by the so far negative searches for lepton flavour violating (LFV) processes, e.g. $\mu \to e\,\gamma$. However, such an assumption may be too restrictive. Furthermore, it has been shown that LFV terms can be induced in the slepton sector even in the constrained MSSM (for vanishing LFV soft SUSY breaking terms at the GUT scale) when supplemented with right-handed neutrino superfields for accommodating neutrino data [4]. These LFV terms can give rise to LFV SUSY particle reactions at an observable level. For the ILC, LFV reactions in SUSY particle productions and decays have been studied for the cases of two generation mixings $\tilde{e} - \tilde{\mu}$ [5, 6, 7, 8, 9], $\tilde{\mu} - \tilde{\tau}$ [10], and $\tilde{e} - \tilde{\tau}$ [11, 12]. Moreover, the case of three generation mixing $\tilde{e} - \tilde{\mu} - \tilde{\tau}$ has been studied in [11, 13, 14, 15, 16, 17, 18] (in [14, 19] also for a muon collider). Some of the studies above, i.e. [11, 13, 14, 16, 18], are rather model dependent. In contrast, our framework is the general MSSM, where we impose no further assumptions other than important experimental and theoretical requirements which have to be respected by the MSSM parameters. Furthermore, so far no systematic study of LFV in sneutrino decays including bosonic decays has been performed. The aim of this article is to perform a systematic study of sneutrino production and decays including the bosonic decay modes in the general MSSM with LFV in slepton sector. We study the cases of two generation mixings in the slepton sector, i.e. $\tilde{\mu} - \tilde{\tau}$ and $\tilde{e} - \tilde{\tau}$ mixings. We do not expect significant LFV effects in sneutrino decays in the $\tilde{e} - \tilde{\mu}$ mixing case [8]. We show that the LFV sneutrino production cross sections and the LFV decay branching ratios for both fermionic and bosonic sneutrino decays can be quite large due to slepton generation mixing in a significant part of the MSSM parameter space despite the very strong experimental limits on LFV processes. This could have an important impact on the search for sneutrinos and the MSSM parameter determination at future colliders, such as LHC, ILC, CLIC and muon collider.

In section 2 we give an account on slepton generation mixing in the general MSSM. In Section 3 we list the constraints which we impose on the model parameters. Our numerical analysis on LFV sneutrino production and decays is given in section 4. We summarize in

section 5.

2 The model

First we summarize the MSSM parameters in our analysis. The most general charged slepton mass matrix including left-right mixing as well as flavour mixing in the basis of $\tilde{\ell}_{0\alpha} = (\tilde{e}_L, \tilde{\mu}_L, \tilde{\tau}_L, \tilde{e}_R, \tilde{\mu}_R, \tilde{\tau}_R)$, $\alpha = 1, ..., 6$, is given by [17, 20]:

$$M^2_{\tilde{\ell}} = \begin{pmatrix} M^2_{LL} & M^{2\dagger}_{RL} \\ M^2_{RL} & M^2_{RR} \end{pmatrix} , \tag{1}$$

where the entries are 3×3 matrices. They are given by

$$\begin{aligned} M^2_{LL,\alpha\beta} &= M^2_{L,\alpha\beta} + m_Z^2 \cos(2\beta)(-\frac{1}{2} + \sin^2\theta_W)\delta_{\alpha\beta} + m^2_{\ell_\alpha}\delta_{\alpha\beta} , & (2)\\ M^2_{RR,\alpha\beta} &= M^2_{E,\alpha\beta} - m_Z^2 \cos(2\beta)\sin^2\theta_W\delta_{\alpha\beta} + m^2_{\ell_\alpha}\delta_{\alpha\beta} , & (3)\\ M^2_{RL,\alpha\beta} &= v_1 A_{\beta\alpha} - m_{\ell_\alpha}\mu^* \tan\beta\delta_{\alpha\beta} . & (4) \end{aligned}$$

The indices $\alpha, \beta = 1, 2, 3$ characterize the flavours e, μ, τ, respectively. M^2_L and M^2_E are the hermitean soft SUSY breaking mass matrices for left and right sleptons, respectively. $A_{\alpha\beta}$ are the trilinear soft SUSY breaking couplings of the sleptons and the Higgs boson: $\mathcal{L}_{\rm int} = -A_{\alpha\beta}\tilde{\ell}^\dagger_{\beta R}\tilde{\ell}_{\alpha L}H^0_1 + A_{\alpha\beta}\tilde{\ell}^\dagger_{\beta R}\tilde{\nu}_{\alpha L}H^-_1 + \cdots$. μ is the higgsino mass parameter. v_1 and v_2 are the vacuum expectation values of the Higgs fields with $v_1 = \langle H^0_1\rangle$, $v_2 = \langle H^0_2\rangle$, and $\tan\beta \equiv v_2/v_1$. We work in a basis where the Yukawa coupling matrix $Y_{E,\alpha\beta}$ of the charged leptons is real and flavour diagonal with $Y_{E,\alpha\alpha} = m_{\ell_\alpha}/v_1 = \frac{g}{\sqrt{2}}\frac{m_{\ell_\alpha}}{m_W\cos\beta}$ ($\ell_\alpha = e, \mu, \tau$), with m_{ℓ_α} being the physical lepton masses and g the SU(2) gauge coupling. The physical mass eigenstates $\tilde{\ell}_i$, $i = 1, ..., 6$, are given by $\tilde{\ell}_i = R^{\tilde{\ell}}_{i\alpha}\tilde{\ell}_{0\alpha}$. The mixing matrix $R^{\tilde{\ell}}$ and the physical mass eigenvalues are obtained by an unitary transformation $R^{\tilde{\ell}}M^2_{\tilde{\ell}}R^{\tilde{\ell}\dagger} = \mathrm{diag}(m^2_{\tilde{\ell}_1}, \ldots, m^2_{\tilde{\ell}_6})$, where $m_{\tilde{\ell}_i} < m_{\tilde{\ell}_j}$ for $i < j$. Similarly, the mass matrix for the sneutrinos, in the basis $\tilde{\nu}_{0\alpha} = (\tilde{\nu}_{eL}, \tilde{\nu}_{\mu L}, \tilde{\nu}_{\tau L}) \equiv (\tilde{\nu}_e, \tilde{\nu}_\mu, \tilde{\nu}_\tau)$, reads

$$M^2_{\tilde{\nu},\alpha\beta} = M^2_{L,\alpha\beta} + \frac{1}{2}m_Z^2\cos(2\beta)\delta_{\alpha\beta} \qquad (\alpha, \beta = 1, 2, 3) , \tag{5}$$

where the physical mass eigenstates are given by $\tilde{\nu}_i = R^{\tilde{\nu}}_{i\alpha}\tilde{\nu}_{0\alpha}$, $i = 1, 2, 3$, ($m_{\tilde{\nu}_1} < m_{\tilde{\nu}_2} < m_{\tilde{\nu}_3}$).

The properties of the charginos $\tilde{\chi}^\pm_i$ ($i = 1, 2$, $m_{\tilde{\chi}^\pm_1} < m_{\tilde{\chi}^\pm_2}$) and neutralinos $\tilde{\chi}^0_k$ ($k = 1, ..., 4$, $m_{\tilde{\chi}^0_1} < ... < m_{\tilde{\chi}^0_4}$) are determined by the parameters M_2, M_1, μ and $\tan\beta$, where M_2 and M_1 are the SU(2) and U(1) gaugino masses, respectively. Assuming gaugino mass unification we take $M_1 = (5/3)\tan^2\theta_W M_2$.

The possible fermionic and bosonic two-body decay modes of sneutrinos are

$$\begin{aligned} \tilde{\nu}_i &\longrightarrow \nu\tilde{\chi}^0_j,\ \ell^-_\alpha\tilde{\chi}^+_k , & (6)\\ \tilde{\nu}_i &\longrightarrow \tilde{\ell}^-_j W^+,\ \tilde{\ell}^-_j H^+ . & (7) \end{aligned}$$

Note that the neutrino flavour cannot be discriminated in high energy collider experiments. The bosonic decays in (7) are possible if the mass splitting between sneutrinos and sleptons is sufficiently large. We have used the formulas for the partial decay widths as given in [3] by appropriately modifying the couplings to inculde flavour violation as given, for instance, in [20].

3 Constraints

In our analysis, we impose the following conditions on the MSSM parameter space in order to respect experimental and theoretical constraints:

(i) The vacuum stability conditions [21]: $|A_{\alpha\alpha}|^2 < 3\, Y^2_{E,\alpha\alpha}(M^2_{L,\alpha\alpha} + M^2_{E,\alpha\alpha} + m_1^2)$, and $|A_{\alpha\beta}|^2 < Y^2_{E,\gamma\gamma}(M^2_{L,\alpha\alpha} + M^2_{E,\beta\beta} + m_1^2)$, $(\alpha \neq \beta; \gamma = Max(\alpha,\beta); \alpha,\beta = 1,2,3 = e,\mu,\tau)$ where $m_1^2 = (m^2_{H^+} + m_Z^2 \sin^2\theta_W)\sin^2\beta - \frac{1}{2}\, m_Z^2$.

(ii) Experimental limits on the LFV lepton decays: $B(\mu^- \to e^-\gamma) < 1.2 \times 10^{-11}$ (90% CL) [22], $B(\tau^- \to \mu^-\gamma) < 4.5 \times 10^{-8}$ (90% CL) [23], $B(\tau^- \to e^-\gamma) < 1.1 \times 10^{-7}$ (90% CL) [24], $B(\mu^- \to e^-e^+e^-) < 1.0 \times 10^{-12}$ (90% CL) [25], $B(\tau^- \to \mu^-\mu^+\mu^-) < 3.2 \times 10^{-8}$ (90% CL) [26], $B(\tau^- \to e^-e^+e^-) < 3.6 \times 10^{-8}$ (90% CL) [26].

(iii) Experimental limits on SUSY contributions to anomalous magnetic moments of leptons [27, 28] [1]: $|\Delta a_e^{SUSY}| < 7.4 \times 10^{-12}$ (95% CL), $|\Delta a_\mu^{SUSY} - 287 \times 10^{-11}| < 178 \times 10^{-11}$ (95% CL), $|\Delta a_\tau^{SUSY}| < 0.033$ (95% CL).

(iv) The LEP limits on SUSY particle masses [29, 30]: $m_{\tilde{\chi}_1^\pm} > 103$ GeV, $m_{\tilde{\chi}_1^0} > 50$ GeV, $m_{\tilde{\ell}_1} > 100$ GeV, $m_{\tilde{\ell}_1} > m_{\tilde{\chi}_1^0}$, $m^2_{H^+} \gtrsim m_A^2 + m_W^2 > (93\text{ GeV})^2 + (80\text{ GeV})^2 = (123\text{ GeV})^2$.

(v) The limit on m_{H^+} and $\tan\beta$ from the experimental data on $B(B_u^- \to \tau^-\bar{\nu}_\tau)$ [31] [2]: $|R^{SUSY}_{B\tau\nu} - 1.13| < 1.04$ (95% CL) with $R^{SUSY}_{B\tau\nu} \equiv B^{SUSY}(B_u^- \to \tau^-\bar{\nu}_\tau)/B^{SM}(B_u^- \to \tau^-\bar{\nu}_\tau) \simeq (1 - (\frac{m_{B^+}\tan\beta}{m_{H^+}})^2)^2$.

We use the one-loop formulas from [34, 35] for the computation of the SUSY contributions to the observables in conditions (ii) (for $\ell^- \to \ell'^-\gamma$) and (iii). It has been shown that in general the limit on the $\mu^- - e^-$ conversion rate is respected if the limit on $\mu \to e\,\gamma$ is fulfilled [34]. For the calculation of the LFV three-body decay modes in (ii) we use

[1] For anomalous magnetic moments of electron and tau lepton (a_e and a_τ) we take an experimental error range at 95% CL for the SUSY contributions Δa_e^{SUSY} and Δa_τ^{SUSY} using the data of [27]. Also for the limit on Δa_μ^{SUSY}, we allow for an error at 95% CL for the difference between the experimental measurement and the SM prediction [28].

[2] The Babar experiment also has obtained similar data on $B(B_u^+ \to \tau^+\nu_\tau)$ [32] (see also [33]). We have checked that our scenarios studied in this article are allowd also by this data.

the formulas given in [36]. When calculating $B^{SUSY}(B_u^- \to \tau^- \bar{\nu}_\tau)$ in (v) we use the tree-level formula [37], where only the W^- and H^- exchanges contribute, as we do not specify the squark-gluino sector. There are no further constraints on the basic MSSM parameters in our study from the other observables in the B-meson sector, like $B(b \to s\gamma)$, $B(B_s^0 \to \mu^+\mu^-)$ and ΔM_{B_s}, since the slepton sector is essentially independent of the squark-gluino sector in our framework of the general MSSM.

Condition (i) is a necessary condition for the tree-level vacuum stability [21]. This condition strongly constrains the trilinear couplings $A_{\alpha\beta}$, especially for small $\tan\beta$ where the lepton Yukawa couplings $Y_{E,\alpha\alpha}$ are small. For the limits on the lepton flavour mixing parameters $A_{\alpha\beta}$ ($\alpha \neq \beta$) we find that now the experimental limits on them from LFV lepton processes in (ii) can be stronger than the theoretical limits from the vacuum stability condition (i) depending on parameter regions (see [21]). (ii) strongly constrains the lepton flavour mixing parameters; e.g. in case of $\tilde{\mu}-\tilde{\tau}$ mixing the limit on $B(\tau^- \to \mu^-\gamma)$ strongly constrains the $\tilde{\mu}-\tilde{\tau}$ mixing parameters $M^2_{L,23}$, $M^2_{E,23}$, A_{23} and A_{32}. (v) strongly constrains m_{H^+} and $\tan\beta$. The limit on Δa_μ^{SUSY} in (iii) is also important, e.g. it disfavours negative μ especially for large $\tan\beta$.

4 Numerical results

We take $\tan\beta, m_{H^+}, M_2, \mu, M^2_{L,\alpha\beta}, M^2_{E,\alpha\beta}$, and $A_{\alpha\beta}$ as the basic MSSM parameters at the weak scale. We assume them to be real. The LFV parameters are $M^2_{L,\alpha\beta}, M^2_{E,\alpha\beta}$, and $A_{\alpha\beta}$ with $\alpha \neq \beta$. First we study in detail $\tilde{\mu} - \tilde{\tau}$ mixing with the parameters as given in Table 1. This scenario is within the reach of LHC and ILC and satisfies the conditions (i)-(v). For the branching ratios of the LFV leptonic two-body decays we obtain $B(\mu^- \to e^-\gamma) = 1.59 \times 10^{-14}$, $B(\tau^- \to \mu^-\gamma) = 2.35 \times 10^{-8}$, and $B(\tau^- \to e^-\gamma) = 2.71 \times 10^{-15}$. The branching ratios for the LFV leptonic three-body decays are calculated to be $B(\mu^- \to e^-e^+e^-) = 9.7 \times 10^{-17}$, $B(\tau^- \to e^-e^+e^-) = 2.9 \times 10^{-17}$, and $B(\tau^- \to \mu^-\mu^+\mu^-) = 5.4 \times 10^{-11}$. The SUSY contributions to the anomalous magnetic moments of the leptons are calculated to be $\Delta a_e^{SUSY} = 2.82\times10^{-14}$, $\Delta a_\mu^{SUSY} = 1.24\times10^{-9}$, and $\Delta a_\tau^{SUSY} = 3.40 \times 10^{-7}$. The resulting chargino and neutralino masses are given by $m_{\tilde{\chi}_1^\pm} = 147$ GeV, $m_{\tilde{\chi}_2^\pm} = 661$ GeV and $m_{\tilde{\chi}_1^0} = 138$ GeV, $m_{\tilde{\chi}_2^0} = 155$ GeV, $m_{\tilde{\chi}_3^0} = 331$ GeV, $m_{\tilde{\chi}_4^0} = 661$ GeV, respectively. In Table 2 the slepton mass spectrum and the corresponding decompositions in flavour eigenstates are given.

The $\tilde{\nu}_1$ and $\tilde{\nu}_2$ two-body decay branching ratios are displayed in Table 3. As $\tilde{\nu}_2 \sim \tilde{\nu}_\mu$ and $\tilde{\ell}_1^- \sim \tilde{\tau}_R^-$, the decays $\tilde{\nu}_2 \to \tau^-\tilde{\chi}_1^+$ and $\tilde{\nu}_2 \to \tilde{\ell}_1^- H^+$ are essentially LFV decays. Note that the branching ratios of these LFV decays are sizable in this scenario. The reason is as follows: The lighter neutralinos $\tilde{\chi}^0_{1,2}$ and the lighter chargino $\tilde{\chi}_1^\pm$ are dominantly higgsinos as $M_{1,2} \gg |\mu|$ in this scenario. Hence the fermionic decays into $\tilde{\chi}^0_{1,2}$ and $\tilde{\chi}_1^+$ are suppressed by the small lepton Yukawa couplings except for the decay into $\tau^-\tilde{\chi}_1^+$ which does not receive such a suppression because of the sizable τ Yukawa coupling $Y_{E,33}$ for

M_2	μ	$\tan\beta$	m_{H^+}
650	150	20	150

$M^2_{L,\alpha\beta}$	$\beta=1$	$\beta=2$	$\beta=3$
$\alpha=1$	$(430)^2$	1	1
$\alpha=2$	1	$(410)^2$	$(61.2)^2$
$\alpha=3$	1	$(61.2)^2$	$(400)^2$

$A_{\alpha\beta}$	$\beta=1$	$\beta=2$	$\beta=3$
$\alpha=1$	0	0	0
$\alpha=2$	0	0	25
$\alpha=3$	0	0	150

$M^2_{E,\alpha\beta}$	$\beta=1$	$\beta=2$	$\beta=3$
$\alpha=1$	$(230)^2$	1	1
$\alpha=2$	1	$(210)^2$	$(22.4)^2$
$\alpha=3$	1	$(22.4)^2$	$(200)^2$

Table 1: MSSM parameters in our $\tilde{\mu}-\tilde{\tau}$ mixing scenario. All mass parameters are given in GeV.

$R^{\tilde{\nu}}_{i\alpha}$	$\tilde{\nu}_e$	$\tilde{\nu}_\mu$	$\tilde{\nu}_\tau$	Mass
$\tilde{\nu}_1$	0.0	-0.36	0.93	393
$\tilde{\nu}_2$	0.0	0.93	0.36	407
$\tilde{\nu}_3$	1.0	0.0	0.0	425

$R^{\tilde{\ell}}_{i\alpha}$	$\tilde{e}_L$	$\tilde{\mu}_L$	$\tilde{\tau}_L$	$\tilde{e}_R$	$\tilde{\mu}_R$	$\tilde{\tau}_R$	Mass
$\tilde{\ell}_1$	0.0	-0.003	0.033	0.0	-0.12	0.99	204
$\tilde{\ell}_2$	0.0	0.002	0.004	0.0	0.99	0.12	215
$\tilde{\ell}_3$	0.0	0.0	0.0	1.0	0.0	0.0	234

Table 2: Sneutrino and charged slepton compositions, i.e. the mixing matrices $R^{\tilde{\nu}}_{i\alpha}$ and $R^{\tilde{\ell}}_{i\alpha}$ for $i=1,2,3$, and the associated mass spectra (in GeV) for the scenario of Table 1.

$B(\tilde{\nu}_1\to\nu\tilde{\chi}^0_1)=0.066$	$B(\tilde{\nu}_1\to\nu\tilde{\chi}^0_2)=0.016$	$B(\tilde{\nu}_1\to\nu\tilde{\chi}^0_3)=0.045$
$B(\tilde{\nu}_1\to\mu^-\tilde{\chi}^+_1)=0.014$	$B(\tilde{\nu}_1\to\tau^-\tilde{\chi}^+_1)=0.36$	
$B(\tilde{\nu}_1\to\tilde{\ell}^-_1W^+)=0.015$	$B(\tilde{\nu}_1\to\tilde{\ell}^-_1H^+)=0.48$	
$B(\tilde{\nu}_2\to\nu\tilde{\chi}^0_1)=0.14$	$B(\tilde{\nu}_2\to\nu\tilde{\chi}^0_2)=0.034$	$B(\tilde{\nu}_2\to\nu\tilde{\chi}^0_3)=0.13$
$B(\tilde{\nu}_2\to\mu^-\tilde{\chi}^+_1)=0.20$	$B(\tilde{\nu}_2\to\tau^-\tilde{\chi}^+_1)=0.12$	$B(\tilde{\nu}_2\to\tilde{\ell}^-_1H^+)=0.38$

Table 3: Branching ratios of $\tilde{\nu}_1$ and $\tilde{\nu}_2$ decays in the scenario of Table 1. Branching ratios smaller than 1% are not shown.

large $\tan\beta$. This leads to an enhancement of the bosonic decays into the Higgs boson H^+. Moreover the decay $\tilde{\nu}_2(\sim\tilde{\nu}_\mu)\to\tilde{\ell}^-_1(\sim\tilde{\tau}^-_R)+H^+$ is enhanced by the sizable trilinear $\tilde{\nu}_\mu-\tilde{\tau}^+_R-H^-_1$ coupling A_{23} (with $H^-_1=H^-\sin\beta$). Because of the sizable $\tilde{\nu}_\mu-\tilde{\nu}_\tau$ mixing term $M^2_{L,23}$ the $\tilde{\nu}_2$ has a significant $\tilde{\nu}_\tau$ component, which results in a further enhancement of this decay due to the large trilinear $\tilde{\nu}_\tau-\tilde{\tau}^+_R-H^-_1$ coupling A_{33} ($=150$ GeV).
Similarly the decay $\tilde{\nu}_1(\sim\tilde{\nu}_\tau)\to\tilde{\ell}^-_1(\sim\tilde{\tau}^-_R)+H^+$ is enhanced by the large A_{33}. The decays of $\tilde{\nu}_1(\sim\tilde{\nu}_\tau)$ and $\tilde{\nu}_2(\sim\tilde{\nu}_\mu)$ into $\tilde{\ell}^-_2(\sim\tilde{\mu}^-_R)+H^+$ are suppressed due to the vanishing trilinear couplings A_{32} and A_{22}, respectively. The decays into $\tilde{\ell}^-_{1,2}W^+$ are suppressed since $\tilde{\ell}^-_1\sim\tilde{\tau}^-_R$ and $\tilde{\ell}^-_2\sim\tilde{\mu}^-_R$.

In experimental searches for LFV in sneutrino decays it is important to have at least two different lepton-flavour modes with sizable branching ratios in decay of a sneutrino; e.g. *both* sizable $B(\tilde{\nu}_2 \to \mu^- \tilde{\chi}_1^+)$ *and* sizable $B(\tilde{\nu}_2 \to \tau^- \tilde{\chi}_1^+)$. To allow for an experimental distinction of the branching ratios of $\tilde{\nu}_1$, $\tilde{\nu}_2$ and $\tilde{\nu}_3$, sufficiently large mass differences among the three sneutrinos are required. However, large $\tilde{\nu}$ mass differences tend to lead to small $\tilde{\nu}$ generation mixing angles such as θ_{23}^{eff} (i.e. small LFV effects), where the effective $\tilde{\nu}_\mu - \tilde{\nu}_\tau$ mixing angle θ_{23}^{eff} is defined by $\tan(2\theta_{23}^{eff}) \equiv 2M_{L,23}^2/(M_{L,22}^2 - M_{L,33}^2)$ with $M_{L,22}^2 - M_{L,33}^2 \sim m_{\tilde{\nu}_2}^2 - m_{\tilde{\nu}_1}^2$ for the scenario given in Table 1.

4.1 $\tilde{\nu}$ decay branching ratios

We study the basic MSSM parameter dependences of the LFV sneutrino decay branching ratios for the reference scenario of Table 1. In Fig.1 we show contours of $\tilde{\nu}_2$ decay branching ratios in the $\mu - M_2$ plane. All basic parameters other than μ and M_2 are fixed as in our scenario defined in Table 1. We see that the LFV decay branching ratios $B(\tilde{\nu}_2 \to \tau^- \tilde{\chi}_1^+)$ and $B(\tilde{\nu}_2 \to \tilde{\ell}_1^- H^+)$ can be sizable in a significant part of the $\mu - M_2$ plane. The main reason for the increase of $B(\tilde{\nu}_2 \to \tilde{\ell}_1^- H^+)$ in the region $M_2 \gg \mu$ is that the partial widths for the decays into $\mu^- \tilde{\chi}_1^+$ and $\nu \tilde{\chi}_{1,2}^0$ decrease for increasing $|M_2/\mu|$ as the lighter chargino/neutralino states become more and more higgsino like. The $\tau^- \tilde{\chi}_1^+$ decay mode has a different behaviour due to the sizable τ Yukawa coupling for large $\tan\beta$. We remark that the limit on Δa_μ^{SUSY} excludes the region with $B(\tilde{\nu}_2 \to \tilde{\ell}_1^- H^+) \gtrsim 0.5$. For the LFV $\tilde{\nu}_1$ decay we obtain $B(\tilde{\nu}_1 \to \mu^- \tilde{\chi}_1^+) = (0.015, 0.03, 0.05)$ for (μ, M_2) (GeV) $= (200, 600), (400, 360), (600, 280)$, respectively.
In the following we use the quantities $R_{L23} \equiv M_{L,23}^2/((M_{L,11}^2 + M_{L,22}^2 + M_{L,33}^2)/3)$ and $R_{A23} \equiv A_{23}/((|A_{11}| + |A_{22}| + |A_{33}|)/3)$ as a measure of LFV. In Fig.2 we present the R_{L23} dependence of $\tilde{\nu}_2$ decay branching ratios, where all basic parameters other than $M_{L,23}^2$ are fixed as in the scenario specified in Table 1. We see that the LFV decay branching ratios $B(\tilde{\nu}_2 \to \tau^- \tilde{\chi}_1^+)$ and $B(\tilde{\nu}_2 \to \tilde{\ell}_1^- H^+)$ can be large and very sensitive to R_{L23}. Note that $\tilde{\ell}_1^- \sim \tilde{\tau}_R^-$ and that the $\tilde{\nu}_\tau$ component in $\tilde{\nu}_2 (\sim \tilde{\nu}_\mu)$ increases with the increase of the $\tilde{\nu}_\mu - \tilde{\nu}_\tau$ mixing parameter $M_{L,23}^2$, which explains the behaviour of the branching ratios. Similarly we have found that $B(\tilde{\nu}_2 \to \tilde{\ell}_1^- H^+)$ can be very sensitive to R_{A23}; this decay can be enhanced also by a sizable A_{23} as explained above. To exemplify this behaviour further, in Fig.3 we show the contours of these decay branching ratios in the $R_{L23} - R_{A23}$ plane, where all basic parameters other than $M_{L,23}^2$ and A_{23} are fixed as in the scenario of Table 1. As can be seen, these LFV decay branching ratios can be large in a sizable region of the $R_{L23} - R_{A23}$ plane and their dependences on R_{L23} and R_{A23} are quite remarkable and very different from each other. Hence, a simultaneous measurement of these two branching ratios could play an important role in the determination of the LFV parameters $M_{L,23}^2$ and A_{23}.
In Fig.4 we show contours of the LFV decay branching ratio $B(\tilde{\nu}_1 \to \tilde{\ell}_2^- H^+)$ in the $R_{E23} - R_{A32}$ plane for our scenario, where $R_{E23} \equiv M_{E,23}^2/((M_{E,11}^2 + M_{E,22}^2 + M_{E,33}^2)/3)$ and $R_{A32} \equiv A_{32}/((|A_{11}| + |A_{22}| + |A_{33}|)/3)$. All basic parameters other than $M_{E,23}^2$ and

$B(\tilde{\nu}_1 \to \nu\tilde{\chi}_1^0) = 0.066$	$B(\tilde{\nu}_1 \to \nu\tilde{\chi}_2^0) = 0.016$	$B(\tilde{\nu}_1 \to \nu\tilde{\chi}_3^0) = 0.043$
$B(\tilde{\nu}_1 \to e^-\tilde{\chi}_1^+) = 0.014$	$B(\tilde{\nu}_1 \to \tau^-\tilde{\chi}_1^+) = 0.37$	
$B(\tilde{\nu}_1 \to \tilde{\ell}_1^- W^+) = 0.015$	$B(\tilde{\nu}_1 \to \tilde{\ell}_1^- H^+) = 0.48$	
$B(\tilde{\nu}_3 \to \nu\tilde{\chi}_1^0) = 0.14$	$B(\tilde{\nu}_3 \to \nu\tilde{\chi}_2^0) = 0.034$	$B(\tilde{\nu}_3 \to \nu\tilde{\chi}_3^0) = 0.12$
$B(\tilde{\nu}_3 \to e^-\tilde{\chi}_1^+) = 0.20$	$B(\tilde{\nu}_3 \to \tau^-\tilde{\chi}_1^+) = 0.12$	$B(\tilde{\nu}_3 \to \tilde{\ell}_1^- H^+) = 0.38$

Table 4: Branching ratios of $\tilde{\nu}_1$ and $\tilde{\nu}_3$ decays in the $\tilde{e} - \tilde{\tau}$ mixing scenario. Branching ratios smaller than 1% are not shown.

A_{32} are fixed as in the scenario described in Table 1. We find that this branching ratio can be large in a sizable region of the $R_{E23} - R_{A32}$ plane, and that it is sensitive to R_{E23} and R_{A32}, which suggests that its measurement may be important for a determination of the LFV parameters $M^2_{E,23}$ and A_{32}. This behaviour of $B(\tilde{\nu}_1 \to \tilde{\ell}_2^- H^+)$ can be explained as follows: the decay $\tilde{\nu}_1(\sim \tilde{\nu}_\tau) \to \tilde{\ell}_2^-(\sim \tilde{\mu}_R^-) + H^+$ can be enhanced by a sizable trilinear $\tilde{\nu}_\tau - \tilde{\mu}_R^+ - H_1^-$ coupling A_{32}. Moreover, for a sizable $\tilde{\mu}_R - \tilde{\tau}_R$ mixing term $M^2_{E,23}$, $\tilde{\ell}_2^-$ has a significant $\tilde{\tau}_R^-$ component, which leads to an enhancement of this decay due to the large trilinear $\tilde{\nu}_\tau - \tilde{\tau}_R^+ - H_1^-$ coupling A_{33}.
In Fig.5 we show a scatter plot of LFV decay branching ratios $B(\tilde{\nu}_2 \to \tilde{\ell}_1^- H^+)$ versus $B(\tau^- \to \mu^-\gamma)$ for the scenario of Table 1 where the parameters M_2, μ, R_{L23}, R_{E23}, R_{A23} and R_{A32} are randomly generated in the ranges $0 < M_2 < 1000\,GeV$, $|\mu| < 1000\,GeV$, $|R_{L23}| < 0.1$, $|R_{E23}| < 0.2$, $|R_{A23}| < 2.5$ and $|R_{A32}| < 2.5$ (corresponding to $|M^2_{L,23}| < (131\,GeV)^2$, $|M^2_{E,23}| < (96\,GeV)^2$, $|A_{23}| < 125\,GeV$ and $|A_{32}| < 125\,GeV$). All parameters other than $M_2, \mu, M^2_{L,23}, M^2_{E,23}, A_{23}$ and A_{32} are fixed as given in Table 1. As can be seen in Fig.5, the LFV branching ratio $B(\tilde{\nu}_2 \to \tilde{\ell}_1^- H^+)$ could go up to 30% even if the present bound on $B(\tau^- \to \mu^-\gamma)$ improves by one order of magnitude. For the other LFV decay branching ratios of $\tilde{\nu}_{1,2}$ versus $B(\tau^- \to \mu^-\gamma)$ we have obtained scatter plots similar to that for $B(\tilde{\nu}_2 \to \tilde{\ell}_1^- H^+)$ versus $B(\tau^- \to \mu^-\gamma)$, with the upper limits of the $\tilde{\nu}_{1,2}$ decay branching ratios $B(\tilde{\nu}_1 \to \mu^-\tilde{\chi}_1^+) \lesssim 0.12$, $B(\tilde{\nu}_1 \to \tilde{\ell}_2^- H^+) \lesssim 0.40$, $B(\tilde{\nu}_1 \to \tilde{\ell}_2^- W^+) \lesssim 0.05$, $B(\tilde{\nu}_2 \to \tau^-\tilde{\chi}_1^+) \lesssim 0.35$, and $B(\tilde{\nu}_2 \to \tilde{\ell}_1^- W^+) \lesssim 0.22$. Note that $B(\tilde{\nu}_1 \to \tilde{\ell}_2^- H^+)$ can be very large due to sizable $M^2_{E,23}$, A_{32} and large A_{33}, as explained above. $B(\tilde{\nu}_1 \to \mu^-\tilde{\chi}_1^+)$ can be significant for sizable M^2_{L23} and $M_2 \ll |\mu|$ where $\tilde{\nu}_1$ has a sizable $\tilde{\nu}_\mu$ component and $\tilde{\chi}_1^+$ is mainly gaugino-like. $B(\tilde{\nu}_2 \to \tilde{\ell}_1^- W^+)$ can be sizable by the following reason: The decay $\tilde{\nu}_2(\sim \tilde{\nu}_\mu) \to \tilde{\ell}_1^-(\sim \tilde{\tau}_R^-) + W^+$ can be enhanced by a sizable $\tilde{\mu}_L - \tilde{\tau}_R$ mixing parameter A_{23} which leads to a sizable $\tilde{\mu}_L$ component in $\tilde{\ell}_1$. This decay can also be enhanced by a sizable $\tilde{\nu}_\mu - \tilde{\nu}_\tau$ mixing parameter $M^2_{L,23}$ which leads to a sizable $\tilde{\nu}_\tau$ component in $\tilde{\nu}_2$; the $\tilde{\nu}_\tau$ component can couple to W^+ and to the sizable $\tilde{\tau}_L$ component in $\tilde{\ell}_1$ which is due to the large $\tilde{\tau}_L - \tilde{\tau}_R$ mixing term $M^2_{RL,33}$ (for large $|\mu| \tan\beta$), see Eq. (4). Similarly $B(\tilde{\nu}_1 \to \tilde{\ell}_2^- W^+)$ can be enhanced by a sizable A_{32}.

We have also studied the influence of LFV on the sneutrino decay branching ratios for the case of $\tilde{e} - \tilde{\tau}$ mixing, where the MSSM parameters are taken as in Table 1 modified

by the changes: $M^2_{L,11} = (410\ \mathrm{GeV})^2$, $M^2_{L,22} = (405\ \mathrm{GeV})^2$, $M^2_{L,33} = (400\ \mathrm{GeV})^2$, $M^2_{L,23} \leftrightarrow M^2_{L,13}$ and $A_{23} \leftrightarrow A_{13}$. Then $\tilde{\nu}_1 \sim \tilde{\nu}_\tau$, $\tilde{\nu}_2 \approx \tilde{\nu}_\mu$ and $\tilde{\nu}_3 \sim \tilde{\nu}_e$, where the corresponding masses are $m_{\tilde{\nu}_1} = 393$ GeV, $m_{\tilde{\nu}_2} = 400$ GeV and $m_{\tilde{\nu}_3} = 407$ GeV, respectively. The resulting $\tilde{\nu}_1$ and $\tilde{\nu}_3$ decay branching ratios are given in Table 4. As can be seen, these branching ratios are similar to the corresponding ones in the $\tilde{\mu} - \tilde{\tau}$ mixing scenario of Table 1, e.g. $B(\tilde{\nu}_3 \to e^- \tilde{\chi}^+_1)$ in the $\tilde{e} - \tilde{\tau}$ mixing scenario has the same value as $B(\tilde{\nu}_2 \to \mu^- \tilde{\chi}^+_1)$ in the $\tilde{\mu} - \tilde{\tau}$ mixing scenario. We have also found that the dependences of the decay branching ratios on the LFV parameters are similar (including the excluded regions) to those in the $\tilde{\mu} - \tilde{\tau}$ mixing scenario. For instance, $B(\tilde{\nu}_3 \to \tau^- \tilde{\chi}^+_1)$ shows a similar dependence on R_{L13} ($\equiv M^2_{L,13}/((M^2_{L,11} + M^2_{L,22} + M^2_{L,33})/3)$) to that of $B(\tilde{\nu}_2 \to \tau^- \tilde{\chi}^+_1)$ on R_{L23} shown in Fig.2. This is due to the fact that $Y_{E,11} \sim Y_{E,22} (\sim 0)$, that the experimental limits on $B(\tau^- \to e^- \gamma)$ and $B(\tau^- \to \mu^- \gamma)$ are comparable, and that the theoretical constraints on the LFV parameters A_{13} and A_{31} from condition (i) are also similar to those on A_{23} and A_{32}.

4.2 $\tilde{\nu}$ production cross sections

It is to be noted that the production cross sections $\sigma(e^+e^- \to \tilde{\nu}_i \bar{\tilde{\nu}}_j) \equiv \sigma_{ij}$ for $i \neq j$ with $i, j = 1, 2, 3$ are negligible in the $\tilde{\mu} - \tilde{\tau}$ mixing scenario of Table 1. This is due to the fact that in this scenario the t-channel chargino exchanges contribute significantly only to σ_{33} (with $\tilde{\nu}_3 \approx \tilde{\nu}_e$). Furthermore, the s-channel Z boson exchange cannot contribute to the cross section for $i \neq j$ because of the vanishing $Z\tilde{\nu}_i \bar{\tilde{\nu}}_j$ couplings, which is due to the unitarity of the mixing matrix $R^{\tilde{\nu}}$. For the same reason the dependence of the cross sections σ_{ii} with $i = 1, 2, 3$ on the LFV parameter $M^2_{L,23}$ is very weak in this scenario.

In the $\tilde{e} - \tilde{\tau}$ mixing scenario, however, the influence of slepton generation mixing on $\sigma(e^+e^- \to \tilde{\nu}_i \bar{\tilde{\nu}}_j)$ is completely different from that in the $\tilde{\mu} - \tilde{\tau}$ mixing scenario. The reason is that in the $\tilde{e} - \tilde{\tau}$ mixing scenario the t-channel chargino exchanges contribute significantly to the cross sections σ_{ij} for i, j =1,3, enhancing the cross sections strongly and yielding pronounced dependences of the cross sections on the $\tilde{\nu}_e - \tilde{\nu}_\tau$ mixing parameter $M^2_{L,13}$. Note that $\tilde{\nu}_1$ ($\tilde{\nu}_3$) is mainly $\tilde{\nu}_\tau$ ($\tilde{\nu}_e$) with a small $\tilde{\nu}_e$ ($\tilde{\nu}_\tau$) component.
In Fig.6 we show the R_{L13} dependence of σ_{11}, σ_{13} (= σ_{31}) and σ_{33} at $\sqrt{s} = 1$ TeV for longitudinal polarization of -90% and 60% of the electron and positron beam, respectively. All parameters other than $M^2_{L,13}$ are fixed as in our $\tilde{e} - \tilde{\tau}$ mixing scenario described in subsection 4.1. We remark that the production of a pair of sneutrinos with different masses is a unique signal of LFV. This cross section σ_{13} (= σ_{31}) can be as large as about 17fb in this scenario as can be seen in Fig.6. The analysis of [39] shows that the sneutrino mass can be measured with an error of about 0.6 % at ILC. In our case this corresponds to a mass uncertainty of about 2.5 GeV and hence the expected mass difference $m_{\tilde{\nu}_3} - m_{\tilde{\nu}_1}$ of about 10 GeV should be measurable at ILC.

4.3 LFV contributions to collider signatures

Now we study the LFV contributions to signatures of sneutrino production and decay at the ILC. At e^+e^- colliders the experimental sensitivity to $\tilde{e}-\tilde{\tau}$ mixing is in general larger than that to $\tilde{\mu}-\tilde{\tau}$ mixing because of the larger sneutrino production cross sections due to the sizable t-channel chargino exchange contributions [11]. Therefore, we first discuss signatures in the $\tilde{e}-\tilde{\tau}$ mixing scenario described in subsection 4.1. We calculate the LFV contributions in sneutrino production and decay to the rate of the signal events

$$e^{\pm}\tau^{\mp} + 4\text{jets} + \not{E} \qquad \text{and} \qquad e^{\pm}\tau^{\pm}\tau^{\mp} + 2\text{jets} + \not{E} \; , \tag{8}$$

where $\not{E}$ is the missing energy [3]. We assume $\sqrt{s} = 1$ TeV and a longidutinal polarization of -90% and 60% for the electron and positron beam, respectively. From Table 4 we see that the dominant LFV contributions to the rate of the signal event $e^{\pm}\tau^{\mp} + 4\text{jets} + \not{E}$ is obtained by [4]

$$\begin{aligned} \sigma_1^{LFV} &= \sigma_1 \cdot \sum_q B(\tilde{\chi}_1^+ \to q\bar{q}'\tilde{\chi}_1^0) \cdot \sum_q B(\tilde{\chi}_1^- \to q\bar{q}'\tilde{\chi}_1^0) \; , \\ \sigma_1 &= 2 \sum_{i=1}^{3}\sum_{j=1}^{3} \sigma(e^+e^- \to \tilde{\nu}_i\bar{\tilde{\nu}}_j)\; B(\tilde{\nu}_i \to \tau^-\tilde{\chi}_1^+)\; B(\bar{\tilde{\nu}}_j \to e^+\tilde{\chi}_1^-) \; , \end{aligned} \tag{9}$$

which we calculate using the program SPheno [38]. The factor 2 in Eq. (9) is due to the summation over the charges of the involved leptons. For the cross sections $\sigma_{ij} \equiv \sigma(e^+e^- \to \tilde{\nu}_i\bar{\tilde{\nu}}_j)$ we obtain $\sigma_{11} = 14$fb, $\sigma_{22} = 5$fb, $\sigma_{33} = 99$fb, $\sigma_{13} = \sigma_{31} = 10$fb, $\sigma_{12} = \sigma_{21} = \sigma_{23} = \sigma_{32} = 0$. Further we get $\sum_q B(\tilde{\chi}_1^{\pm} \to q\bar{q}'\tilde{\chi}_1^0) = 0.67$ in this scenario. As a result, the corresponding cross section that gives rise to $e^{\pm}\tau^{\mp} + 4\text{jets} + \not{E}$ is $\sigma_1^{LFV} = 6.6$fb. Note however that lepton flavour conserving (LFC) transitions also can contribute to the final state $e^{\pm}\tau^{\mp} + 4\text{jets} + \not{E}$. The dominant contribution of this type stems from the reaction $e^+e^- \to \tilde{\nu}_3\bar{\tilde{\nu}}_3$, followed by the LFC decays $\tilde{\nu}_3 \to e^-\tilde{\chi}_1^+$ and $\tilde{\chi}_1^+ \to \tau^+\nu\tilde{\chi}_1^0$, with the branching ratio $B(\tilde{\chi}_1^+ \to \tau^+\nu\tilde{\chi}_1^0) = 0.1$. The other $\bar{\tilde{\nu}}_3$ decays as $\bar{\tilde{\nu}}_3 \to \bar{\nu}\tilde{\chi}_3^0$, where subsequently the $\tilde{\chi}_3^0$ decays into $Z\tilde{\chi}_2^0$ (with a branching ratio (BR) of 6%) and into $W^{\mp}\tilde{\chi}_1^{\pm}$ (with BR of 9.3%). Both decay chains lead to a final state containing 4jets plus missing energy, where for the various decay branching ratios we have $\sum_q B(Z \to q\bar{q}) = 0.7$, $\sum_q B(\tilde{\chi}_2^0 \to q\bar{q}\tilde{\chi}_1^0) = 0.62$ and $\sum_q B(W \to q\bar{q}') = 0.68$. Taking into account the branching ratios in the decay chains and summing over the charges of the involved particles, we find that the corresponding cross section is $\sigma_1^{LFC} = 0.033$fb, which is two orders of magnitude smaller than σ_1^{LFV}. One can expect that the kinematical distributions of LFV and LFC contributions are quite different. Hence suitable kinematical cuts would further enhance the ratio of LFV to LFC contributions.

[3] Note that there are also contributions from LFV transitions in the production and decay of charged sleptons to the signals in (8).

[4] We remark that the effect of sneutrino flavour oscillation is negligible since in the considered scenario we have $m^2_{\tilde{\nu}_i} - m^2_{\tilde{\nu}_j} \gg 1/2(m_{\tilde{\nu}_i}\Gamma_{\tilde{\nu}_i} + m_{\tilde{\nu}_j}\Gamma_{\tilde{\nu}_j})$ for $i > j$ [6]. Hence, the rate of the combined process factorizes into the product of production cross section and decay branching ratios.

Now we consider the LFV transitions which give rise to the event $e^{\pm}\tau^{\pm}\tau^{\mp} + 2\text{jets} + \not{E}$. The dominant LFV contributions to the rate of the events is given by

$$\begin{aligned}
\sigma_2^{LFV} &= \sigma_2 \cdot B(H^+ \to \tau^+\nu) \cdot \sum_q B(\tilde{\chi}_1^- \to q\bar{q}'\tilde{\chi}_1^0) \ , \\
\sigma_2 &= 2 \sum_{i=1}^{3}\sum_{j=1}^{3}\sum_{k=1}^{3} \sigma(e^+e^- \to \tilde{\nu}_i\bar{\tilde{\nu}}_j)\ B(\tilde{\nu}_i \to \tilde{\ell}_k^- H^+) \\
&\quad \times \left[B(\bar{\tilde{\nu}}_j \to e^+\tilde{\chi}_1^-)\ B(\tilde{\ell}_k^- \to \tau^-\tilde{\chi}_1^0) + B(\bar{\tilde{\nu}}_j \to \tau^+\tilde{\chi}_1^-)\ B(\tilde{\ell}_k^- \to e^-\tilde{\chi}_1^0)\right], \quad (10)
\end{aligned}$$

where $B(H^+ \to \tau^+\nu) \approx 1$, $B(\tilde{\ell}_{1,2,3}^- \to e^-\tilde{\chi}_1^0) = (0, 0, 0.89)$ and $B(\tilde{\ell}_{1,2,3}^- \to \tau^-\tilde{\chi}_1^0) = (0.38, 0, 0.006)$. We obtain $\sigma_2^{LFV} = 6.7$fb. Also in this case there are LFC contributions to $e^{\pm}\tau^{\pm}\tau^{\mp} + 2\text{jets} + \not{E}$. The dominant one is due to the reaction $e^+e^- \to \tilde{\nu}_1\bar{\tilde{\nu}}_1$, followed by the LFC decays $\tilde{\nu}_1 \to \tau^-\tilde{\chi}_1^+$ and $\bar{\tilde{\nu}}_1 \to \tau^+\tilde{\chi}_1^-$, where subsequently one chargino decays hadronically and the other chargino decays as $\tilde{\chi}_1^{\pm} \to e^{\pm}\nu\tilde{\chi}_1^0$ with $B(\tilde{\chi}_1^{\pm} \to e^{\pm}\nu\tilde{\chi}_1^0) = 0.12$. The corresponding cross section for this reaction is $\sigma_2^{LFC} = 0.31$fb, which is about a factor $1/20$ smaller than σ_2^{LFV}.

We have also studied the LFV contributions to the rate of the signal events $\mu^{\pm}\tau^{\mp} + 4\text{jets} + \not{E}$ and $\mu^{\pm}\tau^{\pm}\tau^{\mp} + 2\text{jets} + \not{E}$ in the $\tilde{\mu} - \tilde{\tau}$ mixing scenario of Table 1. Taking the branching ratios of Table 3, and using Eqs. (9) and (10) with e replaced by μ in the branching ratios, we obtain the corresponding LFV cross sections $\sigma_1^{LFV} = 0.14$fb and $\sigma_2^{LFV} = 0.23$fb, respectively. Similarly, for the corresponding LFC cross sections we obtain $\sigma_1^{LFC} = 0.0034$fb and $\sigma_2^{LFC} = 0.13$fb, respectively.

The examples above show that the LFV processes (including the LFV bosonic decays also) can contribute significantly to signal event rates at linear colliders. This strongly suggests that one should take into account the possibility of the significant contributions of both the LFV fermionic and bosonic decays in the sneutrino search and should also include the LFV parameters in the determination of the basic SUSY parameters at colliders. It is clear that detailed Monte Carlo studies taking into account background and detector simulations are necessary [5]. However, this is beyond the scope of the present article.

Before closing this section we remark that the slepton generation mixings as discussed here could also significantly affect the production and decays of charged sleptons and that complex phases of the LFV parameters, such as $M_{L,23}^2$, might have an important influence on the sneutrino phenomenology [3]. These topics deserve detailed studies and will be treated in forthcoming papers.

[5] It has been shown [14] that the background stemming from the decay of τ into e/μ, can be reasonably suppressed by suitable cuts on the e/μ energy and/or on the e/μ impact parameter.

5 Summary

We have studied sneutrino decays in the cases of $\tilde{\mu} - \tilde{\tau}$ and $\tilde{e} - \tilde{\tau}$ mixings in the slepton sector. In the case of $\tilde{e} - \tilde{\tau}$ mixing we have obtained similar results to those in the $\tilde{\mu} - \tilde{\tau}$ mixing case since the experimental limit on $B(\tau^- \to e^-\gamma)$ is of the same order of magnitude as the one on $B(\tau^- \to \mu^-\gamma)$. The theoretical limits from the vacuum stability conditions on the LFV parameters A_{13} and A_{31} are also similar to those on A_{23} and A_{32}. In the $\tilde{e} - \tilde{\mu}$ mixing case the LFV effect is much smaller because the experimental limit on $B(\mu^- \to e^-\gamma)$ is much stronger than those on $B(\tau^- \to \mu^-\gamma)$ and $B(\tau^- \to e^-\gamma)$ and the theoretical limits from the vacuum stability conditions on the LFV parameters A_{12} and A_{21} are also much stronger than those on A_{23}, A_{32}, A_{13} and A_{31}.

To conclude, we have performed a systematic study of sneutrino production and decays including both fermionic and bosonic decays in the general MSSM with slepton generation mixings. We have shown that LFV sneutrino production cross sections and LFV sneutrino decay branching ratios can be quite large due to LFV in the slepton sector (i.e. due to slepton generation mixing) in a significant part of the MSSM parameter space despite the very strong experimental limits on LFV processes. This could have an important impact on the search for sneutrinos and the MSSM parameter determination at future colliders, such as LHC, ILC, CLIC and muon collider.

Acknowledgements

K.H. thanks H. Haber for useful comments and continuous encouragement. W.P. thanks E. Arganda and M. J. Herrero for providing the code for the calculation of the branching ratios $B(\tau \to 3\ell)$. This work is supported by the 'Fonds zur Förderung der wissenschaftlichen Forschung' (FWF) of Austria, project No. P18959-N16 and by the German Ministry of Education and Research (BMBF) under contract 05HT6WWA. The authors acknowledge support from EU under the MRTN-CT-2006-035505 network programme.

References

[1] For reviews, see:
H.P. Nilles, Phys. Rep. **110** (1984) 1; H.E. Haber and G.L. Kane, Phys. Rep. **117** (1985) 75; R. Barbieri, Riv. Nuov. Cim. **11** (1988) 1; J. F. Gunion and H. E. Haber, Nucl. Phys. B **272** (1986) 1 [Erratum-ibid. B **402** (1993) 567].

[2] A. Bartl, H. Eberl, K. Hidaka, S. Kraml, T. Kon, W. Majerotto, W. Porod, and Y. Yamada, Phys. Lett. B **460** (1999) 157;

A. Bartl, K. Hidaka, T. Kernreiter, W. Porod, Phys. Lett. B **538** (2002) 137 [arXiv:hep-ph/0204071];
T. Gajdosik, R. M. Godbole and S. Kraml, JHEP **0409** (2004) 051 [arXiv:hep-ph/0405167].

[3] A. Bartl, K. Hidaka, T. Kernreiter and W. Porod, Phys. Rev. D **66** (2002) 115009 [arXiv:hep-ph/0207186].

[4] F. Borzumati and A. Masiero, Phys. Rev. Lett. **57** (1986) 961.

[5] N. V. Krasnikov, Phys. Lett. B **388** (1996) 783 [arXiv:hep-ph/9511464].

[6] N. Arkani-Hamed, H. C. Cheng, J. L. Feng and L. J. Hall, Phys. Rev. Lett. **77** (1996) 1937 [arXiv:hep-ph/9603431].

[7] J. L. Feng, Int. J. Mod. Phys. A **13** (1998) 2319 [arXiv:hep-ph/9803319].

[8] N. Oshimo, Eur. Phys. J. C **39** (2005) 383 [arXiv:hep-ph/0409018];
M. Obara and N. Oshimo, JHEP **0608** (2006) 054 [arXiv:hep-ph/0508269].

[9] F. Deppisch, H. U. Martyn, H. Päs, A. Redelbach and R. Rückl, Talk at Linear Collider Workshop 2004, Paris [arXiv:hep-ph/0408140].

[10] M. Guchait, J. Kalinowski and P. Roy, Eur. Phys. J. C **21** (2001) 163 [arXiv:hep-ph/0103161]; J. Kalinowski, Acta Phys. Polon. B **32** (2001) 3755.

[11] D. Nomura, Phys. Rev. D **64** (2001) 075001 [arXiv:hep-ph/0004256].

[12] K. Hohenwarter-Sodek and T. Kernreiter, JHEP **0706** (2007) 071 [arXiv:0704.2684 [hep-ph]].

[13] M. Hirouchi and M. Tanaka, Phys. Rev. D **58** (1998) 032004 [arXiv:hep-ph/9712532].

[14] J. Hisano, M. M. Nojiri, Y. Shimizu and M. Tanaka, Phys. Rev. D **60** (1999) 055008 [arXiv:hep-ph/9808410].

[15] W. Porod and W. Majerotto, Phys. Rev. D **66** (2002) 015003 [arXiv:hep-ph/0201284].

[16] F. Deppisch, H. Päs, A. Redelbach, R. Rückl and Y. Shimizu, Phys. Rev. D **69** (2004) 054014 [arXiv:hep-ph/0310053].

[17] A. Bartl, K. Hidaka, K. Hohenwarter-Sodek, T. Kernreiter, W. Majerotto, and W. Porod, Eur. Phys. J. C **46** (2006) 783 [arXiv:hep-ph/0510074].

[18] A. Dedes, H. E. Haber and J. Rosiek, arXiv:0707.3718 [hep-ph].

[19] H. C. Cheng, AIP Conf. Proc. **435** (1998) 561 [arXiv:hep-ph/9712427].

[20] D. J. H. Chung, L. L. Everett, G. L. Kane, S. F. King, J. Lykken and L. T. Wang, Phys. Rept. **407** (2005) 1 [arXiv:hep-ph/0312378].

[21] J.A. Casas and S. Dimopoulos, Phys. Lett. B **387** (1996) 107 [arXiv:hep-ph/9606237].

[22] M. L. Brooks *et al.* [MEGA Collaboration], Phys. Rev. Lett. **83**, (1999) 1521 [arXiv:hep-ex/9905013].

[23] K. Abe *et al.* [Belle Collaboration], Proceedings of The 33rd International Conference on High Energy Physics (ICHEP 06), Moscow, Russia, 26 Jul - 2 Aug 2006 [arXiv:hep-ex0609049].

[24] B. Aubert *et al.* [BABAR Collaboration], Phys. Rev. Lett. **96** (2006) 041801 [arXiv:hep-ex/0508012].

[25] U. Bellgardt *et al.* [SINDRUM Collaboration], Nucl. Phys. B **299**, (1988) 1.

[26] K. Abe *et al.* [Belle Collaboration], arXiv:0708.3272 (hep-ex).

[27] W. M. Yao *et al.* [Particle Data Group], J. Phys. G **33** (2006).

[28] F. Jegerlehner, arXiv:hep-ph/0703125.

[29] G. Sguazzoni, Proceedings of the 31st International Conference on High Energy Physics, Amsterdam, The Netherlands, 25 - 31 July 2002, Eds. S. Bentvelson, P. de Jong, J. Koch, E. Laenen, p. 709 [arXiv:hep-ex/0210022]; P. Lutz, the same Proceedings, p. 735.

[30] S. Schael *et al.*, ALEPH Collaboration and DELPHI Collaboration and L3 Collaboration and OPAL Collaborations and LEP Working Group for Higgs Boson Searches, Eur. Phys. J. C **47** (2006) 547.

[31] K. Ikado et al. (Belle Collaboration), Phys. Rev. Lett. **97** (2006) 251802 [arXiv:hep-ex/0604018v3].

[32] B. Aubert et al. (Babar Collaboration), arXiv:0705.1820 (hep-ex).

[33] W. S. Hou, Talk at The 15th International Conference on Supersymmetry and the Unification of Fundamental Interactions, Karlsruhe, July 26 - August 1, 2007.

[34] J. Hisano, T. Moroi, K. Tobe and M. Yamaguchi, Phys. Rev. D **53** (1996) 2442 [arXiv:hep-ph/9510309].

[35] A. Bartl, W. Majerotto, W. Porod and D. Wyler, Phys. Rev. D **68** (2003) 053005 [arXiv:hep-ph/0306050].

[36] E. Arganda and M. J. Herrero, Phys. Rev. D **73** (2006) 055003.

[37] W. S. Hou, Phys. Rev. D **48** (1993) 2342.

[38] W. Porod, Comput. Phys. Commun. **153** (2003) 275 [arXiv:hep-ph/0301101].

[39] A. Freitas, A. von Manteuffel and P. M. Zerwas, Eur. Phys. J. C **40** (2005) 435 [arXiv:hep-ph/0408341].

Figure Captions

Figure 1: Contours of the LFV decay branching ratios (a) $B(\tilde{\nu}_2 \to \tau^- \tilde{\chi}_1^+)$ and (b) $B(\tilde{\nu}_2 \to \tilde{\ell}_1^- H^+)$ in the $\mu - M_2$ plane for our $\tilde{\mu} - \tilde{\tau}$ mixing scenario. All parameters other than μ and M_2 are fixed as in Table 1. The region with no solid contour-lines is excluded by the conditions (i) to (v) given in the text; negative μ region is excluded by the limit on Δa_μ^{SUSY} in (iii). The dashed and dash-dotted lines in (a) show contours of $B(\tau^- \to \mu^- \gamma)$ and Δa_μ^{SUSY}, respectively. Note that (iii) requires $1.09 \times 10^{-9} < \Delta a_\mu^{SUSY} < 4.65 \times 10^{-9}$.

Figure 2: R_{L23} dependence of $\tilde{\nu}_2$ decay branching ratios for our $\tilde{\mu} - \tilde{\tau}$ mixing scenario, where all basic parameters other than $M_{L,23}^2$ are fixed as in Table 1. The shown range of R_{L23} is the whole range allowed by the conditions (i) to (v) given in the text.

Figure 3: Contours of the LFV decay branching ratios (a) $B(\tilde{\nu}_2 \to \tau^- \tilde{\chi}_1^+)$ and (b) $B(\tilde{\nu}_2 \to \tilde{\ell}_1^- H^+)$ in the $R_{L23} - R_{A23}$ plane for our $\tilde{\mu} - \tilde{\tau}$ mixing scenario, where all basic parameters other than $M_{L,23}^2$ and A_{23} are fixed as in Table 1. The region with no solid contours is excluded by the conditions (i) to (v) given in the text. The dashed lines in (a) show contours of $B(\tau^- \to \mu^- \gamma)$.

Figure 4: Contours of the LFV decay branching ratio $B(\tilde{\nu}_1 \to \tilde{\ell}_2^- H^+)$ in the $R_{E23} - R_{A32}$ plane for our $\tilde{\mu} - \tilde{\tau}$ mixing scenario, where all basic parameters other than $M_{E,23}^2$ and A_{32} are fixed as in Table 1. The region with no solid contours is excluded by the conditions (i) to (v) given in the text. The dashed lines show contours of $B(\tau^- \to \mu^- \gamma)$.

Figure 5: Scatter plot of the LFV decay branching ratios $B(\tilde{\nu}_2 \to \tilde{\ell}_1^- H^+)$ versus $B(\tau^- \to \mu^- \gamma)$ for our $\tilde{\mu} - \tilde{\tau}$ mixing scenario with the parameters $M_2, \mu, R_{L23}, R_{E23}, R_{A23}$ and R_{A32} varied in the ranges $0 < M_2 < 1000$ GeV, $|\mu| < 1000$ GeV, $|R_{L23}| < 0.1, |R_{E23}| < 0.2, |R_{A23}| < 2.5$ and $|R_{A32}| < 2.5$, satisfying the conditions (i) to (v) given in the text. All parameters other than $M_2, \mu, M_{L,23}^2, M_{E,23}^2, A_{23}$ and A_{32} are fixed as in Table 1.

Figure 6: Production cross sections $\sigma(e^+e^- \to \tilde{\nu}_1 \bar{\tilde{\nu}}_1)$ (dotted line), $\sigma(e^+e^- \to \tilde{\nu}_1 \bar{\tilde{\nu}}_3)$ $(= \sigma(e^+e^- \to \tilde{\nu}_3 \bar{\tilde{\nu}}_1))$ (solid line) and $\sigma(e^+e^- \to \tilde{\nu}_3 \bar{\tilde{\nu}}_3)$ (dashed line) at $\sqrt{s} = 1$ TeV as a function of R_{L13} for our $\tilde{e} - \tilde{\tau}$ mixing scenario. All parameters other than $M_{L,13}^2$ are fixed as in the $\tilde{e} - \tilde{\tau}$ mixing scenario described in subsection 4.1. The R_{L13} region shown is allowed by the conditions (i) to (v) given in the text.

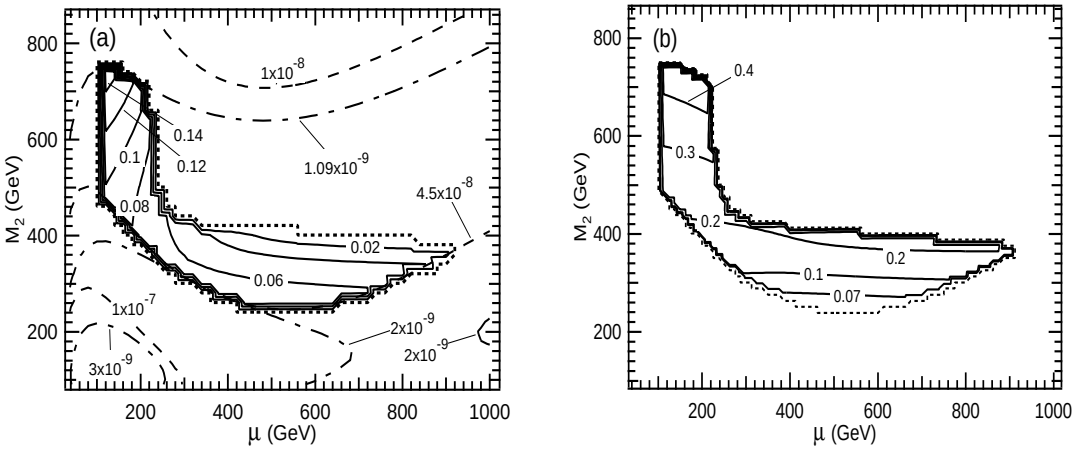
(a)
(b)
M2 (GeV)
μ (GeV)
1x10-8
1.09x10-9
4.5x10-8
0.14
0.12
0.1
0.08
0.02
0.06
1x10-7
3x10-9
2x10-9
2x10-9
0.4
0.3
0.2
0.2
0.1
0.07

Fig.1

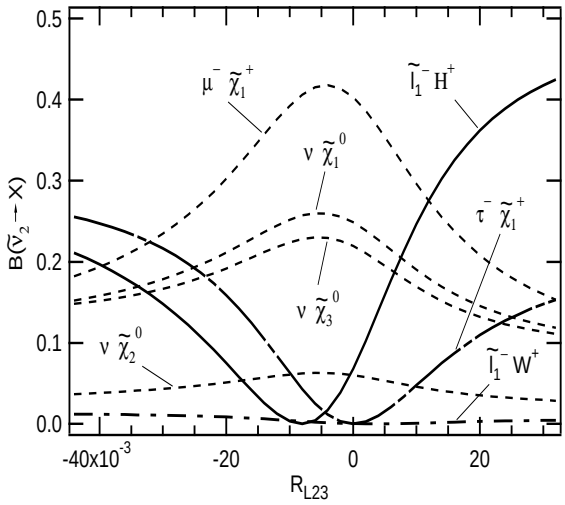
B(ν̃2 → X)
RL23
μ− χ̃1+
ν χ̃1 0
l̃1− H+
τ− χ̃1+
ν χ̃3 0
ν χ̃2 0
l̃1− W+

Fig.2

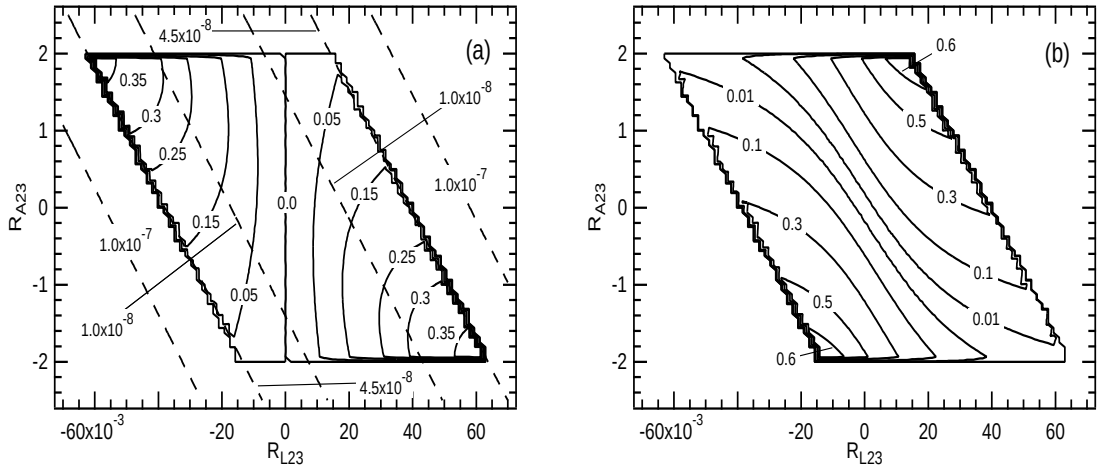
(a)
(b)
R_{A23}
R_{L23}
$4.5x10^{-8}$
$1.0x10^{-8}$
$1.0x10^{-7}$
$-60x10^{-3}$
0.0
0.05
0.15
0.25
0.3
0.35
0.4
0.5
0.6
0.01
0.1

Fig.3

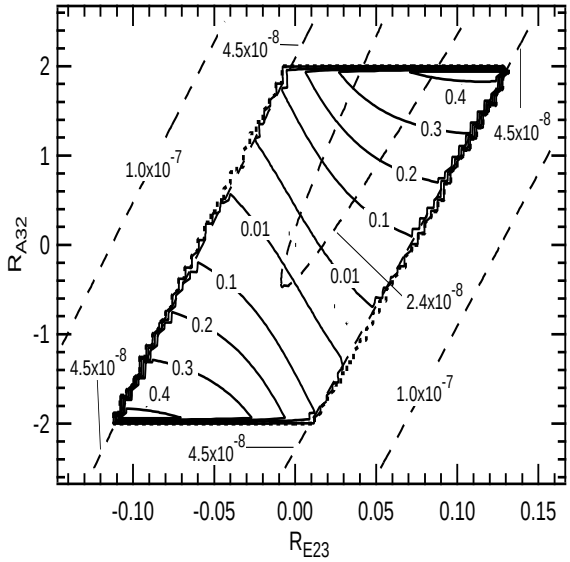
R_{A32}
R_{E23}
$4.5x10^{-8}$
$1.0x10^{-7}$
$2.4x10^{-8}$
0.01
0.1
0.2
0.3
0.4

Fig.4

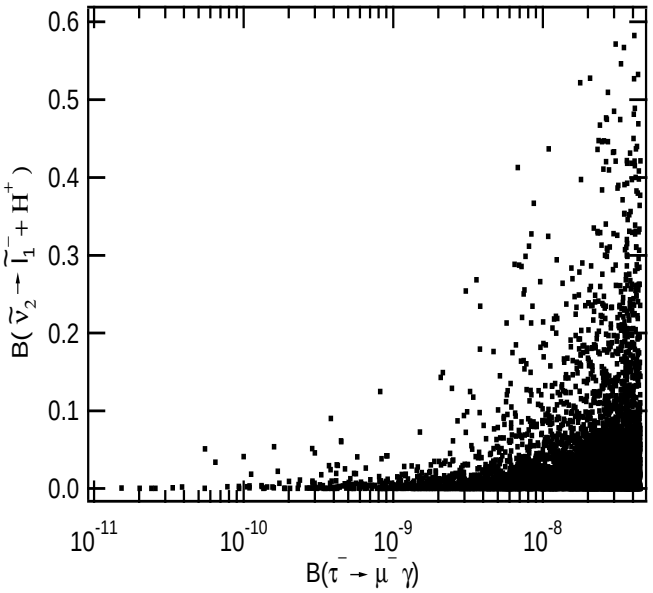
0.6
0.5
0.4
0.3
0.2
0.1
0.0
$B(\tilde{\nu}_2 \to \tilde{l}_1^- + H^+)$
10^{-11}
10^{-10}
10^{-9}
10^{-8}
$B(\tau^- \to \mu^- \gamma)$

Fig.5

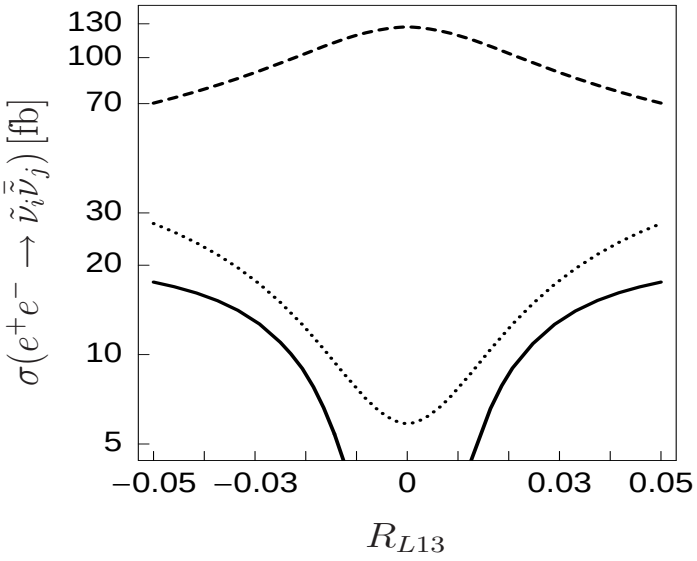
130
100
70
30
20
10
5
$\sigma(e^+e^- \to \tilde{\nu}_i\bar{\tilde{\nu}}_j)$ [fb]
−0.05
−0.03
0
0.03
0.05
R_{L13}

Fig.6